Concepts and Application of *Time-Limiters* to High Resolution Schemes

Karthikeyan Duraisamy,[1] James D. Baeder,[2] and Jian-Guo Liu[3]

Received May 1, 2002; accepted (in revised form) October 20, 2002

A new class of implicit high-order non-oscillatory time integration schemes is introduced in a method-of-lines framework. These schemes can be used in conjunction with an appropriate spatial discretization scheme for the numerical solution of time dependent conservation equations. The main concept behind these schemes is that the order of accuracy in time is dropped locally in regions where the time evolution of the solution is not smooth. By doing this, an attempt is made at locally satisfying monotonicity conditions, while maintaining a high order of accuracy in most of the solution domain. When a linear high order time integration scheme is used along with a high order spatial discretization, enforcement of monotonicity imposes severe time-step restrictions. We propose to apply *limiters* to these time-integration schemes, thus making them non-linear. When these new schemes are used with high order spatial discretizations, solutions remain non-oscillatory for much larger time-steps as compared to linear time integration schemes. Numerical results obtained on scalar conservation equations and systems of conservation equations are highly promising.

KEY WORDS: High resolution schemes; non-linear time integration; time-limiting.

1. INTRODUCTION

In this paper, we consider high resolution numerical schemes for the solution of hyperbolic conservation laws. Currently, the most common approach in the numerical solution of time-dependent partial differential equations is the *method-of-lines*. In this frame-work, spatial discretization is performed over a suitable domain and the resulting system of ordinary differential equations (ODE) in time is solved using standard time-integration schemes. Since this may result in a stiff set of ODE, for many practical applications implicit time integration may be preferred.

Dedicated to Prof. Stanley Osher on the occasion of his 60th birthday.

[1] Graduate Research Student, Department of Aerospace Engineering, University of Maryland, College Park, Maryland 20742.

[2] Associate Professor, Department of Aerospace Engineering, University of Maryland, College Park, Maryland 20742.

[3] Professor, Institute of Physical Science and Technology and Department of Mathematics, University of Maryland, College Park, Maryland 20742. E-mail: jliu@math.umd.edu

0885-7474/03/1200-0139/0

It is well known that solutions of *linear* high order numerical schemes for conservation laws are necessarily non-monotone near regions of discontinuities and high solution gradients. Research on high resolution finite difference and finite volume schemes has mainly concentrated on *controlling* the spatial interpolant. For example, Total Variation Diminishing (TVD) [4] schemes reduce the order of accuracy of spatial interpolation near discontinuities and extrema, the Essentially Non-Oscillatory (ENO) [11] type schemes use an adaptive stencil for spatial interpolation, etc. These approaches essentially make the spatial scheme *non-linear*, thus transcending the restrictions imposed on linear high order schemes.

However, ensuring the non-oscillatory behavior of high order schemes imposes a severe time step restriction. For explicit schemes, this restriction may not be much more severe than the linear stability limit. Gottlieb, Shu, and Tadmor [2] have shown that even implicit time integration schemes (in a method-of-lines framework) become conditionally TVD when the order of accuracy in time is higher than one. In the present work, we review some commonly used implicit schemes from the TVD view-point in a method-of-lines framework. Then we propose concepts of applying *limiters* to popular time integration schemes, thus making them non-linear. The main objective is to enable the use of larger time-steps as compared to linear time integration schemes. This is followed by a demonstration (using a very simple case) of how these schemes exactly work. The final section of the paper presents numerical results and conclusions.

2. MOTIVATION

Consider a scalar conservation law with initial conditions:

$$u_t + f(u)_x = 0, \qquad u(x, 0) = u_o(x) \qquad x \in I, \quad t \in \mathbf{R}^+ \tag{1}$$

For convenience of analysis, we assume $u_o(x)$ to be periodic in a finite interval I. Assuming a spatial grid consisting of volumes $[x_{i-\frac{1}{2}}, x_{i+\frac{1}{2}}]$ and dividing time into intervals $[0, t^1,..., t^n, t^{n+1},...]$, a numerical scheme for Eq. (1) of the form: (Note: $\bar{u}_i^n = \frac{1}{\Delta x}\int_{x_i-\frac{1}{2}}^{x_i+\frac{1}{2}} u(x, t^n)\, dx$)

$$\bar{u}_i^{n+1} = H(\bar{u}_{i-k}^n, \bar{u}_{i-k+1}^n,...., \bar{u}_{i+k}^n) \tag{2}$$

is said to be monotone if

$$\frac{\partial H}{\partial u_j}(u_{i-k}, u_{i-k+1},...., u_{i+k}) \geqslant 0 \qquad \forall i-k \leqslant j \leqslant i+k \tag{3}$$

Harten *et al.* [6] have shown that converged solutions to conservative monotone schemes for Eq. (1) always correspond to physically acceptable states. But it is also well known that monotone schemes for the solution of conservation laws are only of first order of accuracy in space and time. Hence, less restrictive monotonicity conditions are usually used, the most common among which is the Total Variation Diminishing (TVD) condition [4].

The Total Variation of a numerical solution at a time level t^n is defined by,

$$TV(u(.,t^n)) = \sum_{i=-\infty}^{\infty} |u(x_{i+1}, t^n) - u(x_i, t^n)|$$

A numerical scheme for the solution of Eq. (1) is said to be TVD if the Total Variation does not increase in time. That is,

$$TV(u(.,t^{n+1})) \leqslant TV(u(.,t^n))$$

TVD schemes are based on the fact that oscillations always add to the total variation and thus oscillations cannot grow indefinitely if the scheme is TVD [8]. The TVD property is sufficient to guarantee the convergence of a conservative numerical scheme to weak solutions of conservation laws. The TVD condition has the advantage that it is simple to apply and it allows generic high order accuracy without causing spurious oscillations.

The last decade has seen a lot of research in the development of non-oscillatory schemes. Very high order accurate (in space and time) non-oscillatory numerical schemes have been designed and satisfactorily applied in the solution of hyperbolic problems. (For example, the UNO schemes of Harten *et al.* [5], the ENO and WENO [11] schemes, the MP [12] schemes, etc.) But a severe penalty results from the fact that these schemes are non-oscillatory only under severe time-step restrictions. (For example, the 3rd order WENO scheme even for the linear advection equation has to be used with a CFL number less than 0.4 when used with explicit time integration). One way of overcoming this would be to use implicit time integration. But, Gottlieb, Shu, and Tadmor [2] have shown that (in a method-of-lines approach) implicit time integration schemes also become conditionally TVD when the order of accuracy in time is higher than one. Hence the original objective in choosing implicit time integration schemes is lost because of these time-step restrictions.

2.1. TVD Limits for Implicit Schemes

We now review implicit time integration schemes in a method-of-lines framework. This approach is similar to the one due to Shu *et al.* [1], where the analysis is performed for explicit Runge Kutta schemes.

Spatial discretization of Eq. (1) would yield a system of ODEs in time, which, we represent by,

$$u_t = L(u) \tag{4}$$

As mentioned earlier, a large number of highly accurate non-oscillatory spatial discretizations are available in literature. These schemes become conditionally TVD when used with an Euler explicit scheme (which is used as a basis for comparison). Let $\Delta t \leqslant \Delta t_{ee}$ be the allowable time step for which the explicit Euler scheme is TVD. I.e.,

$$\|u^n\| \geqslant \|u^n + \Delta t\, L(u^n)\| \qquad \text{for} \quad \Delta t \leqslant \Delta t_{ee} \tag{5}$$

Note: The norm in question is the Total Variation semi-norm.

Table I. TVD Limits for Some Existing Implicit Schemes

Method[a]	State update formula	k
Imp. Euler	$u^{n+1} = u^n + \Delta t\, L(u^{n+1})$	∞
Imp. Trap	$u^{n+1} = u^n + \frac{\Delta t}{2}[L(u^n) + L(u^{n+1})]$	2.0
Imp. BDF2	$u^{n+1} = \frac{2\Delta t\, L(u^{n+1}) + 4u^n - u^{n-1}}{3}$	0.5
SDIRK-2	$u^{(1)} = u^n + \Delta t \gamma L(u^{(1)})$	
$(\gamma = \frac{2-\sqrt{2}}{2})$	$u^{n+1} = u^n + \Delta t[(1-\gamma)\, L(u^{(1)}) + \gamma L(u^{n+1})]$	$\frac{1}{1-2\gamma} \approx 2.4142$

[a] Imp. BDF2: Implicit Second Order Backward Difference Method, SDIRK-2: 2-Stage Singly Diagonally Implicit Runge Kutta Method.

This provides a good basis for evaluating other time integration schemes for Eq. (4). Hence, any time integration scheme for Eq. (4) would yield a discrete numerical scheme which will be conditionally TVD under a new time step restriction, which we denote by $\Delta t \leqslant k\, \Delta t_{ee}$. Shu *et al.* [1, 2] have carried out an analysis for explicit Runge Kutta (RK) schemes. Shu's results show that $k \leqslant 1$ for high order explicit RK schemes. We extend the same analysis to a few well known implicit schemes. Further, Gottlieb, Shu, and Tadmor have also shown in [2] that implicit RK and implicit multi-step methods of order higher than 1 have finite values of k (or in other words, the resulting numerical schemes are conditionally TVD).

We have derived the value of k for some existing implicit schemes (Table I). The details are given in the appendix. It is seen that only the implicit Euler method (which is first order accurate) is unconditionally TVD. The Trapezoidal method becomes non-monotone for a time-step twice that of the explicit Euler method and the implicit BDF2 becomes non-monotone for half the time-step of the explicit Euler method. The SDIRK-2 which is a 2 stage implicit method performs marginally better than the Trapezoidal method. Hence, it becomes obvious that when these schemes (though they are implicit) are used in the numerical solution of conservation equations, they still have severe time-step restrictions.

3. A NEW CLASS OF IMPLICIT TIME-LIMITED SCHEMES

In this section, 2 new schemes—the Limited-Trapezoidal (L-TRAP) and the Limited-2 Stage Diagonally Implicit Runge–Kutta (L-DIRK2) will be presented.

3.1. The L-TRAP Scheme

Before presenting the details of our new scheme, it is useful to consider the θ method, which is a time-space decoupled method. Consider conservative and consistent numerical flux functions (of any spatial order) corresponding to a non-oscillatory scheme:

$$f^n_{j+\frac{1}{2}} = f(\bar{u}^n_{j-l_1}, \bar{u}^n_{j-l_1+1}, \ldots, \bar{u}^n_{j-l_2-1}, \bar{u}^n_{j-l_2}), \qquad \text{and}$$
$$f^{n+1}_{j+\frac{1}{2}} = f(\bar{u}^{n+1}_{j-l_1}, \bar{u}^{n+1}_{j-l_1+1}, \ldots, \bar{u}^{n+1}_{j-l_2-1}, \bar{u}^{n+1}_{j-l_2}).$$

Table II. Family of Schemes for Fixed Value of θ

Condition	Method	Accuracy	TVD limit (k)
$\theta = 1.0$	Imp. Euler	1st order	∞
$\theta = 0.5$	Imp. Trap	2nd order	2.0
$\theta = 0.0$	Exp. Euler	1st order	1.0

The well-known θ method for the solution of Eq. (1) is given by:

$$\bar{u}_j^{n+1} = \bar{u}_j^n - \tau[(1-\theta)(f^n_{j+\frac{1}{2}} - f^n_{j-\frac{1}{2}}) + \theta(f^{n+1}_{j+\frac{1}{2}} - f^{n+1}_{j-\frac{1}{2}})] \tag{6}$$

On immediate observation, we find that if we fix a constant value of θ over the whole domain, we get the schemes as shown in Table II, and the TVD limit is given by $k = \frac{1}{1-\theta}$.

This scheme can be written in the conservation form,

$$\bar{u}_j^{n+1} = \bar{u}_j^n - \tau(\hat{f}_{j+\frac{1}{2}} - \hat{f}_{j-\frac{1}{2}}), \tag{7}$$

where,

$$\hat{f}_{j\pm\frac{1}{2}} = (1-\theta)\, f^n_{j\pm\frac{1}{2}} + \theta f^{n+1}_{j\pm\frac{1}{2}}$$

We propose a new numerical method, for which:

$$\hat{f}_{j\pm\frac{1}{2}} = (1-\theta_{j\pm\frac{1}{2}})\, f^n_{j\pm\frac{1}{2}} + \theta_{j\pm\frac{1}{2}} f^{n+1}_{j\pm\frac{1}{2}}, \qquad \text{with}$$
$$\theta_{j\pm\frac{1}{2}} = 0.5(\theta_{j\pm1} + \theta_j), \qquad \theta_j, \theta_{j\pm1} \in [0.5, 1]$$

Here, θ_j is a real number between 0.5 and 1.0 and is defined for each cell j (the definition of θ_j is given in the following subsections). Now, since $\hat{f}_{j\pm\frac{1}{2}}$ is a convex combination of conservative and consistent numerical fluxes $f^n_{j\pm\frac{1}{2}}$ and $f^{n+1}_{j\pm\frac{1}{2}}$, it is itself conservative and consistent.

The idea then, is to define a θ_j, such that in regions where the solution is smooth, we would use $\theta_j \approx 0.5$, thus attaining second order accuracy in time locally. In regions of high gradients, we would like a $\theta_j \approx 1.0$, thus locally dropping the time accuracy to first order. By doing this, *an attempt is made at locally satisfying the TVD condition. The definition of θ_j is based on the time evolution of the solution at j, hence this method is no longer fully space-time decoupled.* We term this method the Limited-Trapezoidal method or the L-TRAP.

3.2. The L-DIRK2 Scheme

We propose a new 2-stage implicit scheme for the solution of Eq. (1). The scheme is given by,

$$\bar{u}_j^{(1)} = \bar{u}_j^n - \tau\gamma(f^{(1)}_{j+\frac{1}{2}} - f^{(1)}_{j-\frac{1}{2}})$$
$$\bar{u}_j^{n+1} = \bar{u}_j^n - \tau[(a_{21_{j+\frac{1}{2}}} f^{(1)}_{j+\frac{1}{2}} - a_{21_{j-\frac{1}{2}}} f^{(1)}_{j-\frac{1}{2}}) + (a_{22_{j+\frac{1}{2}}} f^{n+1}_{j+\frac{1}{2}} - a_{22_{j-\frac{1}{2}}} f^{n+1}_{j-\frac{1}{2}})]$$

where,

$$a_{21_{j\pm\frac{1}{2}}} = \gamma + \theta_{j\pm\frac{1}{2}}(1-2\gamma),$$

$$a_{22_{j\pm\frac{1}{2}}} = (1-\gamma) + \theta_{j\pm\frac{1}{2}}(2\gamma-1), \qquad \theta_{j\pm\frac{1}{2}} = 0.5(\theta_j + \theta_{j\pm1}), \quad \theta_j \in [0,1], \quad \gamma = \frac{2-\sqrt{2}}{2}$$

If we keep $\theta_j = \theta$ a constant at all points in the domain, the TVD limit is given by, $k = \frac{1}{\theta(1-2\gamma)}$. It is seen that this scheme reduces to the second order (in time) SDIRK [3] for $\theta = 1.0$ giving a $k = 2.4142$ and to a 2-stage first order unconditionally TVD method if $\theta = 0$. (Refer Appendix for details). Note that both these schemes are in a method-of-lines framework.

Again, the basic idea is to locally drop the order of accuracy in regions of high gradients and maintain second order accuracy in smooth regions. Hence, the local θ_j is defined accordingly.

3.3. Definition of θ_j

The L-TRAP and L-DIRK2 schemes as defined in the previous sections are general and this section presents just one of the ways by which a limiter could be designed.

The definition for θ_j is inspired by the following lemma by Hyunh [7] for quadratic interpolation: *Given the data* $f(q_1)$, $f(q_2)$ *and the derivative* $f'(q_1)$ *or* $f'(q_2)$ *at points* q_1 *and* q_2, *the resulting quadratic interpolant is monotone in* $[q_1, q_2]$ *if* $f'(q_1)$, $f'(q_2) \in [0, 2s]$, *where* $s = \frac{f(q_2)-f(q_1)}{q_2-q_1}$.

Hence, we check whether this monotonicity condition is satisfied (with respect to the time derivative) at all points in the domain. For those points at which this condition is satisfied, we assign $\theta_j \approx 0.5$ for L-TRAP and $\theta_j \approx 1.0$ for L-DIRK2, thus allowing the local time accuracy to be second order. For points at which this condition is not satisfied, a value of θ_j ranging from 0.5 to 1.0 for L-TRAP and θ_j ranging from 1.0 to 0.0 for the L-DIRK2 is assigned. The procedure is as follows:

Let

$$s_j^{n+\frac{1}{2}} = \frac{u_j^{n+1} - u_j^n}{\Delta t}$$

$$L(u_j^n) = \left(\frac{\partial u}{\partial t}\right)_j^n = -\frac{1}{\Delta x}\left(f_{j+\frac{1}{2}}^n - f_{j-\frac{1}{2}}^n\right)$$

$$L(u_j^{n+1}) = \left(\frac{\partial u}{\partial t}\right)_j^{n+1} = -\frac{1}{\Delta x}\left(f_{j+\frac{1}{2}}^{n+1} - f_{j-\frac{1}{2}}^{n+1}\right)$$

Define a parameter r_j for each of the domain points with $\theta_j = 1.0 - 0.5r_j$ for the L-TRAP scheme and $\theta_j = r_j$ for the L-DIRK2 scheme. Hence, $r_j = 1$ for second order accuracy and $r_j = 0$ for first order accuracy.

For monotone quadratic interpolation $L(u_j^n)$ and $L(u_j^{n+1})$ should lie in the interval $[0, 2s_j^{n+\frac{1}{2}}]$. This is true if,

$$L(u_j^{n+1})^* \left(L(u_j^{n+1}) - 2s_j^{n+\frac{1}{2}}\right) \leqslant \epsilon \qquad \text{and} \qquad L(u_j^n)^* \left(L(u_j^n) - 2s_j^{n+\frac{1}{2}}\right) \leqslant \epsilon. \tag{8}$$

$\epsilon = 0$ would strictly be equivalent to the conditions of Hyunh's lemma. An arbitrarily small and positive ϵ (in this case $\epsilon = 1 \times 10^{-10}$) is used to ensure that the limiter does not turn on and off spuriously for small changes in the solution. Hence, *if Eq. (8) is satisfied,* $r_j = 1.0$ *is assigned* and local second order accuracy is approached.

If,

$$\frac{L(u_j^{n+1})}{(s_j^{n+\frac{1}{2}} + \epsilon)} \leqslant -\epsilon_1 \qquad \text{or} \qquad \frac{L(u_j^n)}{(s_j^{n+\frac{1}{2}} + \epsilon)} \leqslant -\epsilon_1 \tag{9}$$

then, either or both of the quantities $L(u_j^n)$ and $L(u_j^{n+1})$ are of the opposite sign as $s_j^{n+\frac{1}{2}}$ and hence the interpolant can become non-monotone. Hence, *if Eq. (9) is satisfied,* $r_j = 0$ *is assigned* and hence the local accuracy is dropped to first order. ϵ_1 is again arbitrarily small and positive. A value of 1×10^{-5} is used.

If Eqs. (8) and (9) are not satisfied, then we have a case which is analogous to a situation where $f'(q_1)$ and $f'(q_2)$ are of the same sign as s, but either or both are too steep. In such a case, an appropriate $r_j \in [0, 1]$ is assigned as follows:

$$r_j = \min\left[\frac{2s_j^{n+\frac{1}{2}}}{L(u_j^n) + \epsilon}, \frac{2s_j^{n+\frac{1}{2}}}{L(u_j^{n+1}) + \epsilon}, 1\right] \tag{10}$$

It becomes clear that $r_j \approx 0$ at discontinuities and at extrema, since these would be indistinguishable by the above procedure. This could introduce undesirable clipping even at smooth extrema. This can be corrected by checking the spatial interpolant. For example, if a MUSCL [13] spatial interpolation is used, we use the strategy developed by Suresh *et al.* in [12] to preserve accuracy near extrema. Given a highly accurate interpolated value at $x_{j+\frac{1}{2}}$, this method determines whether spatial-limiting is required at $x_{j+\frac{1}{2}}$ based on a 4 point spatial stencil. Hence if spatial-limiting is not required for the current solution at $x_{j+\frac{1}{2}}$ at time levels n and $n+1$, r_j is reset to 1.0. Note that if one uses the monotonicity preserving scheme of Suresh *et al.* [12] for spatial discretization, the extra work required to reset the time-limiter is minimal.

4. LINEAR AND NON-LINEAR STABILITY ANALYSIS

We present a linear stability and monotonicity analysis for a simple case. The L-TRAP method is compared with the implicit Euler and Trapezoidal schemes for the linear advection equation $u_t + u_x = 0$ with a first order upwind discretization in periodic space. This discretization is chosen because it is simple, linear and monotone (in a semi-discretized sense). Let the CFL number be represented by $\sigma = \frac{\Delta t}{\Delta x}$ and let the number of spatial points be N. Then, the L-TRAP (and related families of schemes) would be given by:

$$u_j^{n+1} = u_j^n - \sigma[(1 - \theta_{j+\frac{1}{2}})\, u_j^n + \theta_{j+\frac{1}{2}} u_j^{n+1} - (1 - \theta_{j-\frac{1}{2}})\, u_{j-1}^n - \theta_{j-\frac{1}{2}} u_{j-1}^{n+1}]$$

This can be represented in matrix form ($\mathbf{D}[\mathbf{a}, \mathbf{b}]$ is a $N \times N$ periodic bi-diagonal matrix with lower-diagonal elements a_j and diagonal elements b_j):

$$\mathbf{A}[-\sigma\theta_{j-\frac{1}{2}}, 1+\sigma\theta_{j+\frac{1}{2}}]\,\mathbf{U}^{n+1} = \mathbf{B}[\sigma(1-\theta_{j-\frac{1}{2}}), 1-\sigma(1-\theta_{j+\frac{1}{2}})]\,\mathbf{U}^{n}$$

This can be represented as:

$$\mathbf{U}^{n+1} = \mathbf{M}\mathbf{U}^{n}, \qquad \text{where,} \quad \mathbf{M} = \mathbf{A}^{-1}\mathbf{B} \tag{11}$$

Because of the linearity of the problem, one can completely determine the properties of these schemes based on the structure of the matrix $\mathbf{M}$.

4.1. Linear Stability

Since the system is periodic, linear stability is equivalent to the spectral radius of $\mathbf{M}$ being less than 1. For an initial condition consisting of a hat function, ($N = 60$, $\sigma = 3.0$, $t = \Delta t$) Fig. 1 shows the eigen-values of $\mathbf{M}$. Note that $\mathbf{M}$ is a constant matrix for all time-steps for implicit Euler and Trapezoidal methods, whereas, for the L-TRAP case, it changes with time because the limiter is a function of time. It is evident that all 3 schemes are linearly stable. In fact, it is easy to show that all

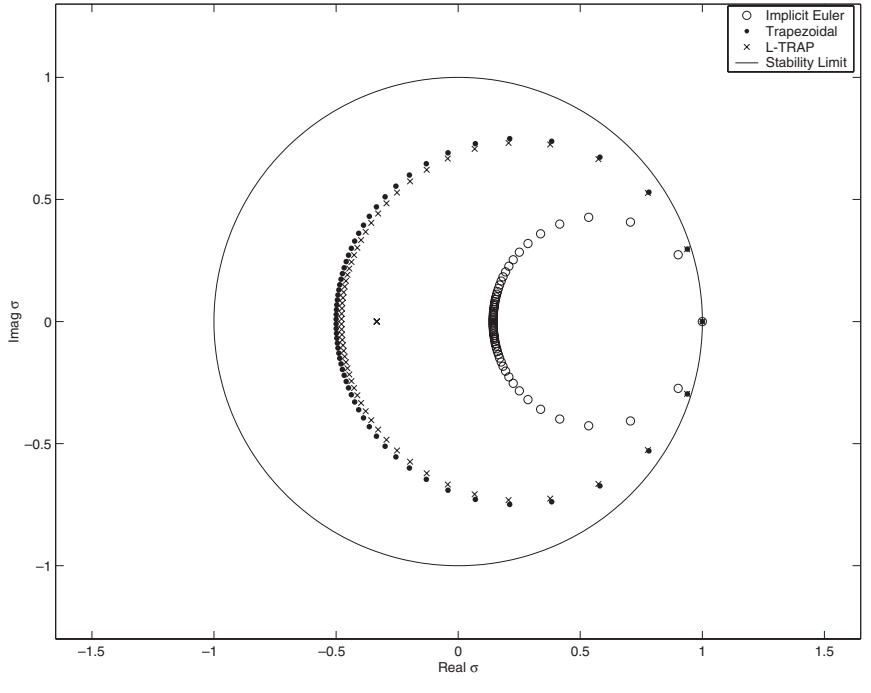

Fig. 1. Eigen-value plot: $\sigma = 3.0$, $N = 60$, $t = \Delta t$.

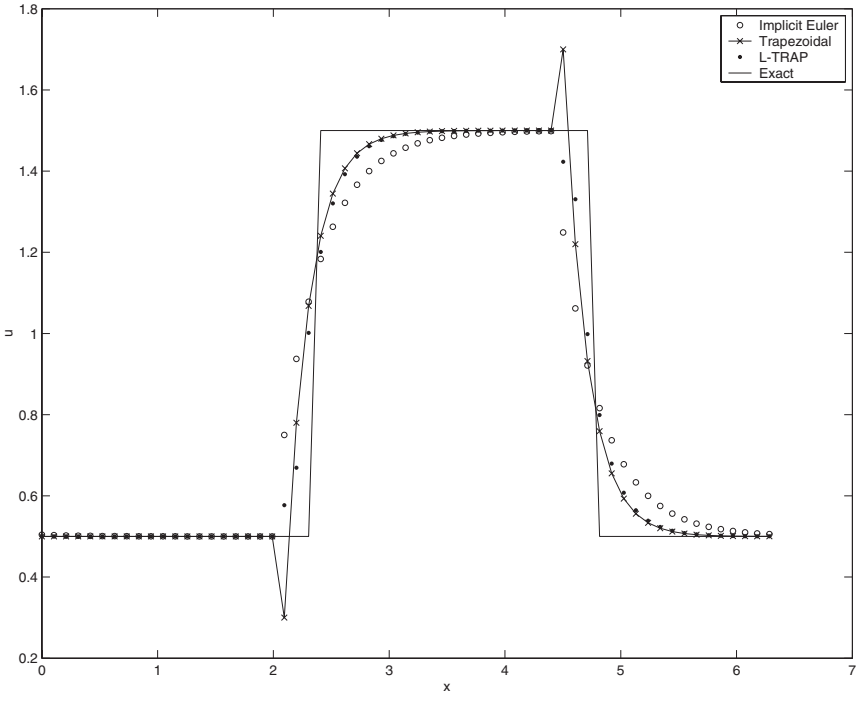

Fig. 2. Numerical Solution: $\sigma = 3.0$, $N = 60$, $t = \Delta t$.

3 schemes are unconditionally linearly stable. This figure gives evidence of the dispersion of the Trapezoidal method and the excessive damping of the implicit Euler method. The L-TRAP method stays close to the Trapezoidal method, except for a pair of eigen-values, which show damping. This is because the limiter (refer Sec. 3.3) senses the sharp discontinuities in time. Figure 2 shows the solution after 1 time step. Since the TVD limit of the Trapezoidal method (with 1st order upwind in space) is $\sigma = 2.0$, it exhibits oscillations in the numerical solution. The L-TRAP scheme stays close to the Trapezoidal method in smooth regions and is thus less dissipative than the implicit Euler method.

4.2. Monotonicity Analysis

Consider Eq. (11). It is then possible to write:

$$u_i^{n+1} = \sum_{j=1}^{N} m_{i,j} u_j^n$$

Now, monotonicity (refer Eq. (3)) is equivalent to ensuring that $m_{i,j} \geqslant 0$, $j = \{1,..., N\}$. It is known that:

- $\sum_{j=1}^{N} m_{i,j} = 1$ from consistency, and
- Therefore, in a global sense, monotonicity is implied by $L^{\infty}(\mathbf{M}) = 1$. If this condition is satisfied, the scheme is rigorously monotone (since along with consistency, this guarantees that $m_{i,j} \geqslant 0 \ \forall i, j$). Hence the numerical solution will be monotone for any initial condition.

However, *this is a sufficient condition and not a necessary one for the monotone behavior of numerical solutions.* For example, if the initial data is smooth the Trapezoidal method would give a smooth solution even if the time-step exceeds the monotonicity limit. Hence, *global monotonicity is not necessary in this case*. The focal point of the above argument is that we can afford to have a non-monotone scheme (but linear stability is still required) in parts of the domain where the solution is smooth and enforce monotonicity in non-smooth regions. In terms of coefficients, this means that $\sum_{j=1}^{N} |m_{i,j}|$ can be > 1 for some i.

On explicit construction of $\mathbf{M}$, it is found that $m_{i,j} \geqslant 0$ for $i \neq j$ for all three methods with 1st order upwinding in space. Also, the Determinant of $\mathbf{A} = |\mathbf{A}|$ is positive. Hence, we need to look at the positivity of only the diagonal elements $m_{i,i}$. We find that these are given by:

$$
\begin{aligned}
m_{i,i} &= \frac{1}{|\mathbf{A}|}\left\{\frac{1-\sigma(1-\theta_{i+\frac{1}{2}})}{1+\sigma\theta_{i+\frac{1}{2}}}\left[\prod_{k=1}^{N}(1+\sigma\theta_{k+\frac{1}{2}})\right]+\frac{\sigma(1-\theta_{i+\frac{1}{2}})}{\sigma\theta_{i+\frac{1}{2}}}\left[\prod_{k=1}^{N}(\sigma\theta_{k+\frac{1}{2}})\right]\right\} \\
&= \frac{1-\sigma(1-\theta_{i+\frac{1}{2}})}{1+\sigma\theta_{i+\frac{1}{2}}}P_1+\frac{\sigma(1-\theta_{i+\frac{1}{2}})}{\sigma\theta_{i+\frac{1}{2}}}P_2, \qquad (\text{clearly, } 0<P_2<P_1) \\
&= \sigma(1-\theta_{i+\frac{1}{2}})\left[\frac{P_2}{\sigma\theta_{i+\frac{1}{2}}}-\frac{P_1}{1+\sigma\theta_{i+\frac{1}{2}}}\right]+\frac{P_1}{1+\sigma\theta_{i+\frac{1}{2}}}
\end{aligned}
$$

From this, we can make the following inferences:

- For the implicit Euler method, $\theta_{i+\frac{1}{2}} = 1 \ \forall i$. Therefore, $m_{i,j} \geqslant 0 \ \forall i, j$. *Hence, $L^{\infty}(\mathbf{M}) = 1$ and this method is unconditionally monotone.*
- For the L-TRAP method, the limiter can ensure that in regions of large gradients, $\theta_{i+\frac{1}{2}} \to 1$ and hence, $m_{i,i} \geqslant 0$ can be maintained. Since $m_{i,j} \geqslant 0$, $i \neq j$, u_i^{n+1} becomes a convex combination of u_j^n, $j = 1,..., N$ and we achieve local monotonicity.
- For the Trapezoidal method, we find that

$$
m_{i,i} = \frac{(1+\frac{\sigma}{2})^{N-1}(1-\frac{\sigma}{2})+(\frac{\sigma}{2})^{N}}{(1+\frac{\sigma}{2})^{N}-(\frac{\sigma}{2})^{N}}
$$

therefore, when $\sigma > 2+\epsilon$, ($\epsilon \to 0$ for large N), $m_{i,i} < 0 \ \forall i$ and the numerical solution becomes non-monotone.

5. NUMERICAL RESULTS

We present numerical results for the linear advection equation, the Burgers' equation and the one dimensional Euler equations. For all the results presented,

LU-SGS [15] with Newton-type sub-iterations [9] is used to solve the implicit set of equations at each time step. Before the start of each sub-iteration, θ_j is determined for all points in the domain and $\theta_{j\pm\frac{1}{2}}$ is updated.

5.1. Linear Advection Equation

The first test case is the linear advection equation $u_t + u_x = 0$, with periodic boundary conditions and a smooth initial condition $u_o(x) = \sin^4(\frac{x}{2})$ over a domain $[0, 2\pi]$. This initial profile is convected one revolution over the uniform domain. The number of spatial points is represented by N. This test case is chosen to demonstrate the fact that smooth extrema are preserved and uniform second order accuracy in time is achieved. A 5th order monotonicity preserving scheme (MP5) [12] is used for spatial discretization. Figure 3 shows the solution after one period of revolution for a domain with $N = 16$ at a CFL number (represented by $\sigma = \frac{\Delta t}{\Delta x}$) of 0.5 using the L-DIRK2 scheme. It is observed that reasonable accuracy is achieved even with this coarse spatial discretization. The extremum is clearly preserved and it is found that the time-limiter sets itself to second order accuracy at all points at all times. Figure 4 shows the L_1, L_2, and L_∞ error norms for the L-TRAP and L-DIRK2 schemes for $\sigma = 0.5$ for different levels of spatial discretizations. It is seen that the errors are within range of $(\Delta t)^2$ and $(\Delta x)^5$. The main observation of this exercise is that the schemes are uniformly second order accurate in time for all evaluated cases and no spurious limiting is present at the smooth extremum.

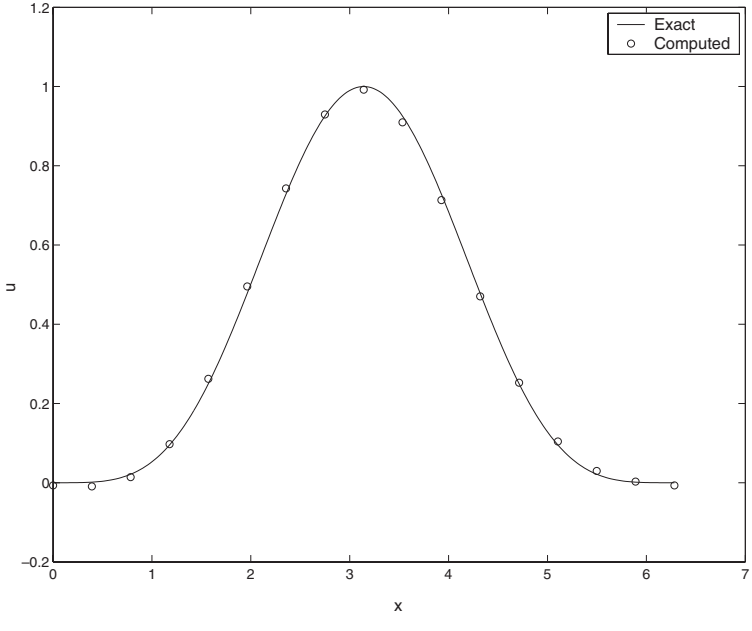

Fig. 3. Linear advection, $\sigma = 0.5$, MP5 in space, $N = 16$, periodic bc, 1 period of rev.

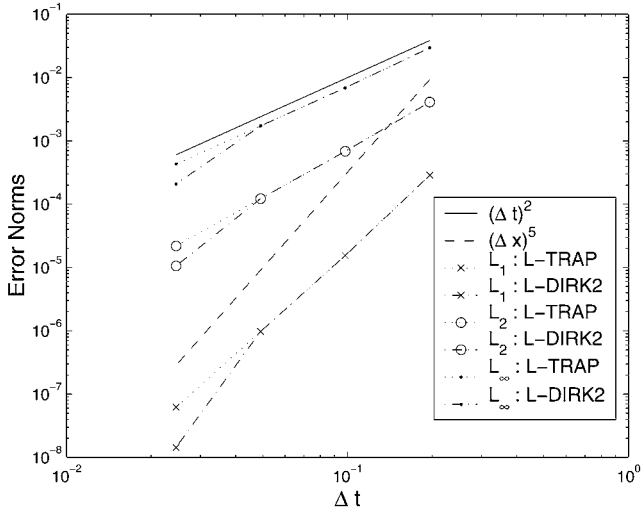

Fig. 4. Error norms for linear advection $\sigma = 0.5$, MP5 in space, periodic bc, 1 period of rev.

The second case is a domain that comprises of a half-sine wave, a step function and a $\sin^4(x)$ distribution over a domain $[0, 2\pi]$, comprising of 360 equally spaced points. This initial condition is convected one revolution over the uniform domain. Spatial discretization is done with the MP5 scheme. The L-TRAP (Fig. 5b) and L-DIRK2 schemes (Fig. 5c) are compared with first and second order implicit schemes. $\sigma = 2.0$ is used because it is high enough to demonstrate the large dissipation exhibited by the first order implicit Euler method and the non-linear instabilities of the second order Trapezoidal and Backward difference methods (Fig. 5a). Note that the CFL number corresponding to the TVD limit $k = 1$ is $\sigma \approx 0.4$ and hence the TVD limit of the Trapezoidal scheme is $\sigma \approx 0.8$ and the limit for the BDF2 is even lower. It is seen that the limited schemes are less dissipative than the first order method and less oscillatory when compared to the linear second order methods.

5.2. Burgers' Equation

The third test case is the inviscid Burgers' equation $u_t + (\frac{u^2}{2})_x = 0$, with periodic boundary conditions and a domain $[0, 2\pi]$ of 100 equally spaced points. The initial condition comprises of an expansion wave and a compression wave. This profile is convected till $t = 2.0$, before which the compression wave becomes a shock. The MP5 spatial discretization scheme is used with $\sigma = \{u\}_{\max} \frac{\Delta t}{\Delta x}$. Again, the implicit Euler (Fig. 6a) method shows large dissipation and the linear second order time integration schemes develop oscillations in the vicinity of the shock. It is seen that the limited schemes resolve the expansion wave and the shock well.

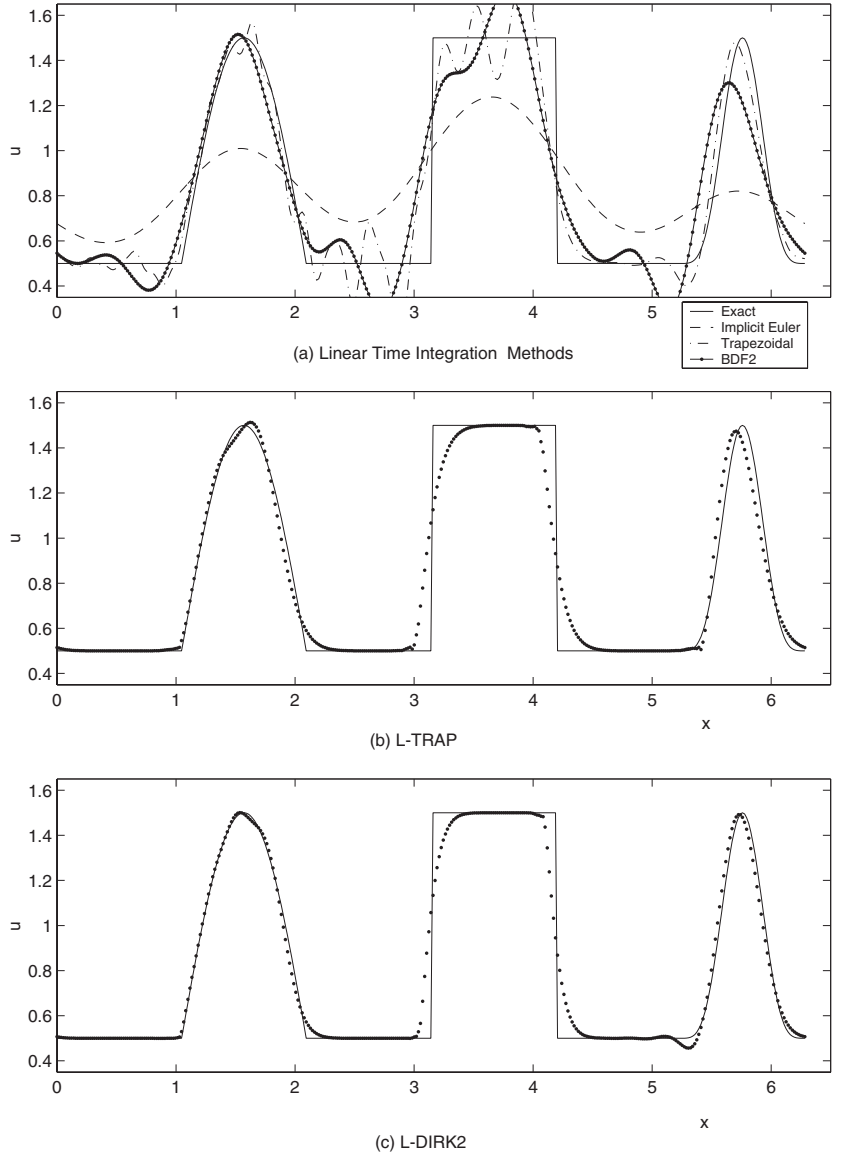

Fig. 5. Linear advection, $\sigma = 2.0$, MP5 in space, $N = 360$, periodic bc, 1 period of rev.

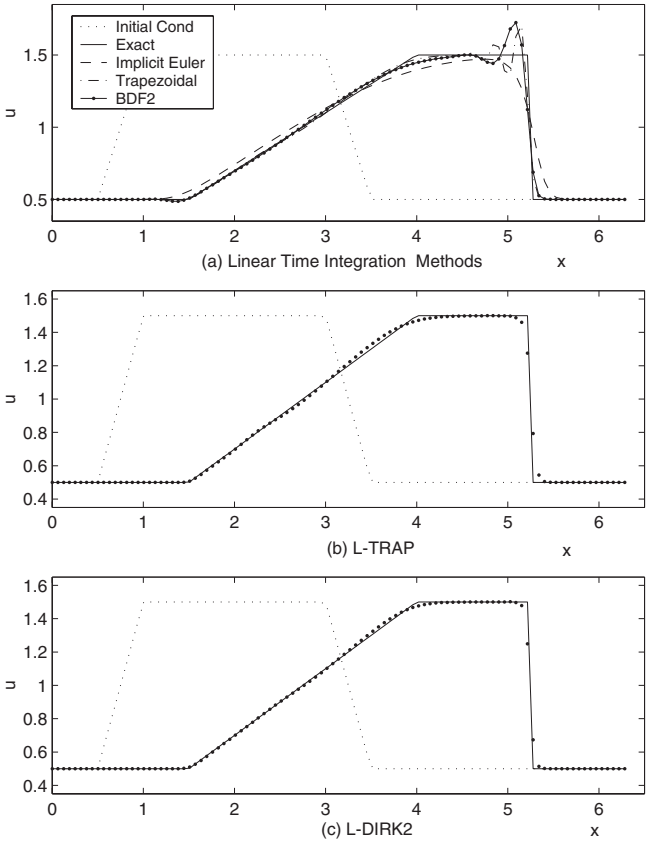

Fig. 6. Burgers' equation, $\sigma = 2.0$, MP5 in space, $N = 100$, periodic bc, $t = 2.0$.

5.3. Euler Equations

The one dimensional Euler equations of gas dynamics are given by:

$$\frac{\partial \mathbf{U}}{\partial t} + \frac{\partial \mathbf{F}}{\partial x} = 0 \tag{12}$$

where $\mathbf{U}$, the vector of conserved variables and $\mathbf{F}$, the flux vector are defined by,

$$\mathbf{U} = \begin{Bmatrix} \rho \\ \rho u \\ e \end{Bmatrix}, \qquad \mathbf{F} = \begin{Bmatrix} \rho u \\ p + \rho u^2 \\ (e+p)\, u \end{Bmatrix}$$

ρ, u, p are density, velocity, and pressure respectively. e is the total energy per unit volume given by,

$$e = \frac{p}{\gamma - 1} + \frac{\rho u^2}{2}$$

The concepts of monotonicity as introduced in the earlier sections of the paper cannot be rigorously defined for a non-linear system of equations like the Euler equations. At best, one can extend the concepts of scalar equations and hope to obtain non-oscillatory numerical solutions.

The limiter r_j in Eqs. (8), (9), and (10) can be defined in many arbitrary ways for a system of equations. For example, in the present work, we have used a density-based limiter, for which,

$$s_j^{n+\frac{1}{2}} = \frac{\rho_j^{n+1} - \rho_j^n}{\Delta t}$$

$$L(\rho_j^n) = \left(\frac{\partial \rho}{\partial t}\right)_j^n = -\frac{1}{\Delta x}\left[(\rho u)_{j+\frac{1}{2}}^n - (\rho u)_{j-\frac{1}{2}}^n\right]$$

$$L(\rho_j^{n+1}) = \left(\frac{\partial \rho}{\partial t}\right)_j^{n+1} = -\frac{1}{\Delta x}\left[(\rho u)_{j+\frac{1}{2}}^{n+1} - (\rho u)_{j-\frac{1}{2}}^{n+1}\right]$$

Since, in a Finite volume framework, these quantities are computed as part of the solution process, these values, when substituted in Eqs. (8), (9), and (10) yield the required limiter. Correction at smooth extrema can also be done using the monotonicity preserving strategy as presented in the previous sections. Note that the time derivative of density is computed using the conservation of mass. Another limiter, for instance, can be defined by using a similar procedure on each of the three conserved variables and choosing the one which is closest to first order.

5.3.1. Implementation

In this section, the implementation of the L-TRAP method in the solution of the one dimensional Euler equations will be presented. Consider a discretization of Eq. (12) with an appropriate high order method for computing the interfacial fluxes $\mathbf{F}_{j\pm\frac{1}{2}}$.

$$\mathbf{U}_j^{n+1} - \mathbf{U}_j^n = -\tau[((1-\theta_{j+\frac{1}{2}})\,\mathbf{F}_{j+\frac{1}{2}}^n - (1-\theta_{j-\frac{1}{2}})\,\mathbf{F}_{j-\frac{1}{2}}^n) + (\theta_{j+\frac{1}{2}}\mathbf{F}_{j+\frac{1}{2}}^{n+1} - \theta_{j-\frac{1}{2}}\mathbf{F}_{j-\frac{1}{2}}^{n+1})] \quad (13)$$

The required implicit term $\mathbf{F}(\mathbf{U}^{n+1})$ can replaced by the upwind-split linear approximation:

$$\mathbf{F}(\mathbf{U}^{n+1}) = \mathbf{F}^+(\mathbf{U}^{n+1}) + \mathbf{F}^-(\mathbf{U}^{n+1})$$

$$\approx [\mathbf{F}^+(\mathbf{U}^n) + \mathbf{A}^+(\mathbf{U}^n)\,\Delta\mathbf{U}^n] + [\mathbf{F}^-(\mathbf{U}^n) + \mathbf{A}^-(\mathbf{U}^n)\,\Delta\mathbf{U}^n]$$

where, $\mathbf{A}^{\pm}$ are approximations to the split-flux Jacobians $\frac{\partial \mathbf{F}^{\pm}}{\partial \mathbf{U}}$. In order to remove linearization errors, one can introduce Newton sub-iterations [9] in the variable p and the set of algebraic equations can be reduced to the form given by:

$$\begin{aligned}
&\Delta\mathbf{U}^p_{j-1}[-\tau\theta_{j-\frac{1}{2}}\mathbf{A}^{+}(\mathbf{U}^n_{j-1})]+\Delta\mathbf{U}^p_j[\mathbf{I}+\tau\theta_{j-\frac{1}{2}}\mathbf{A}^{+}(\mathbf{U}^p_j)-\tau\theta_{j+\frac{1}{2}}\mathbf{A}^{-}(\mathbf{U}^p_j)]\\
&\quad+\Delta\mathbf{U}^p_{j+1}[\tau\theta_{j+\frac{1}{2}}\mathbf{A}^{-}(\mathbf{U}^n_{j+1})]\\
&\quad=-(\mathbf{U}^p_j-\mathbf{U}^n_j)-\tau[((1-\theta_{j+\frac{1}{2}})\,\mathbf{F}^n_{j+\frac{1}{2}}-(1-\theta_{j-\frac{1}{2}})\,\mathbf{F}^n_{j-\frac{1}{2}})+(\theta_{j+\frac{1}{2}}\mathbf{F}^p_{j+\frac{1}{2}}-\theta_{j-\frac{1}{2}}\mathbf{F}^p_{j-\frac{1}{2}})]
\end{aligned}$$

with $\Delta\mathbf{U}^p=\mathbf{U}^{p+1}-\mathbf{U}^p$. Hence a block tridiagonal inversion is required at each sub-iteration p and $\mathbf{U}^{p+1}$ is updated for every sub-iteration as $\mathbf{U}^{p+1}=\mathbf{U}^p+\Delta\mathbf{U}^p$. The sub-iterations are continued till $\|\Delta\mathbf{U}^p\|\to 0$ in a suitable norm, at which point, the RHS is identical to Eq. (13) (with $p=n+1$). Before the start of each sub-iteration, θ_j is determined for all points in the domain. LU-SGS method [15] has been used in the solution of the implicit system of equations. The L-DIRK2 can also be implemented in a similar manner.

5.3.2. Numerical Results

The application of the schemes to the 1-D Euler equations is demonstrated in this section. Both test cases are Riemann problems in a constant area tube. The left and right states are represented by the subscripts L and R. The domain is [0, 1] and the interface is at $x=0.5$. The number of points in the domain is represented by N. Both these solutions do not involve application of boundary conditions since the final time is chosen such that none of the waves cross the computational domain. A second order upwind MUSCL [13] extrapolation is used (with Superbee limiter [10]) for spatial discretization and interfacial fluxes are computed using the AUSMDV [14] flux differencing scheme. The Euler-explicit TVD limit with a Super-bee limiter corresponds to $\sigma=\{|u|+a\}_{\max}\frac{\Delta t}{\Delta x}<0.5$, where u is the local velocity and a is the local sonic velocity.

Sod's Problem. Sod's problem is given by $\{p_L,\rho_L,u_L\}=\{1.0,1.0,0.0\}$ and $\{p_R,\rho_R,u_R\}=\{0.1,0.125,0.0\}$. For this case, $N=200$ and $\sigma=3.0$. Figure 7 shows the density evolution. It is seen that both time-limited methods resolve the expansion wave well and the shock and contact discontinuity are captured without smearing even at this high CFL number. Figure 8 shows the evolution of pressure and reinforces the observations from the density plot.

Lax's Problem. Lax's problem is given by $\{p_L,\rho_L,u_L\}=\{3.528,0.445,0.698\}$ and $\{p_R,\rho_R,u_R\}=\{0.571,0.5,0.0\}$. Figures 9 and 10 demonstrate the results for $N=200$, $\sigma=3.0$.

From these results, it is seen that the L-TRAP and L-DIRK2 methods of time integration are beneficial in the sense that they generate non-oscillatory numerical solutions. Some portions of the solution exhibit very small amplitude oscillations. These can be removed by making improvements on the limiter. We have derived analytical expressions for the TVD limits of the L-TRAP scheme assuming a second order MUSCL spatial discretization. The local time-step restriction appears to be a

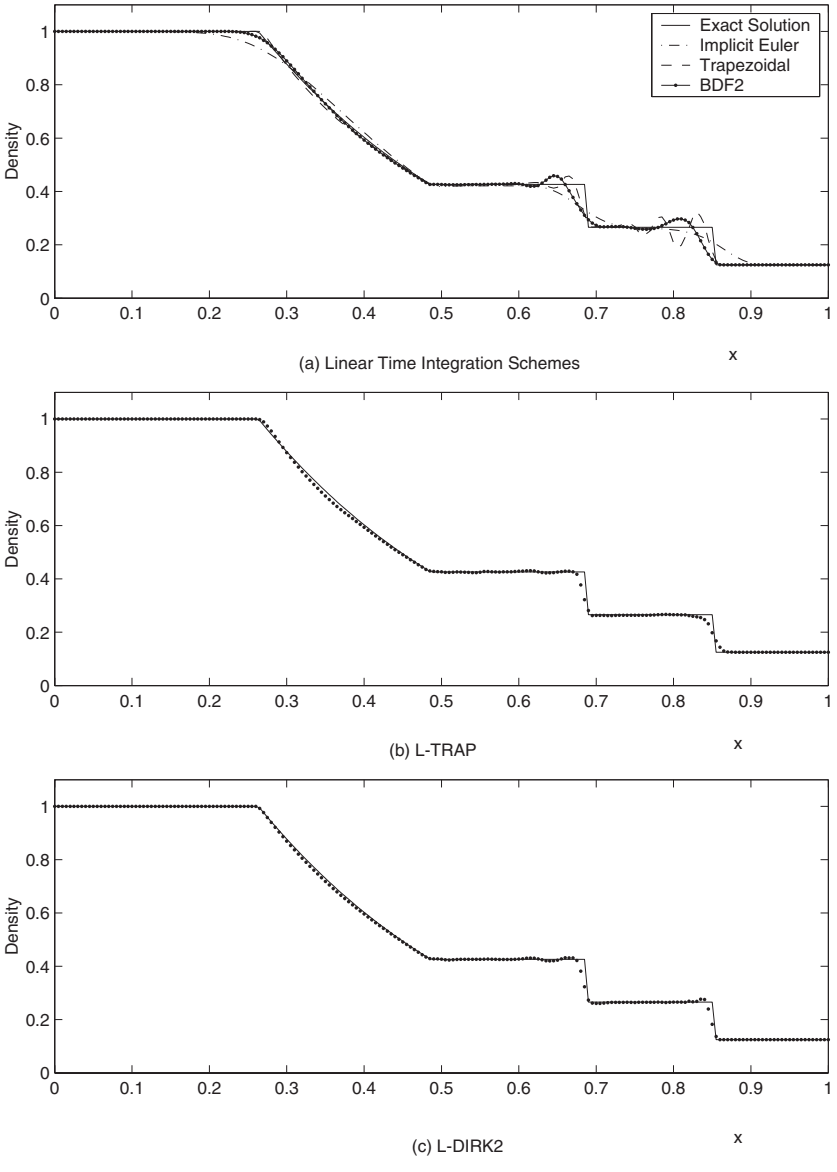

Fig. 7. Sod's problem (Density), $\sigma = 3.0$, 2nd order MUSCL, $N = 200$, $t = 0.2$.

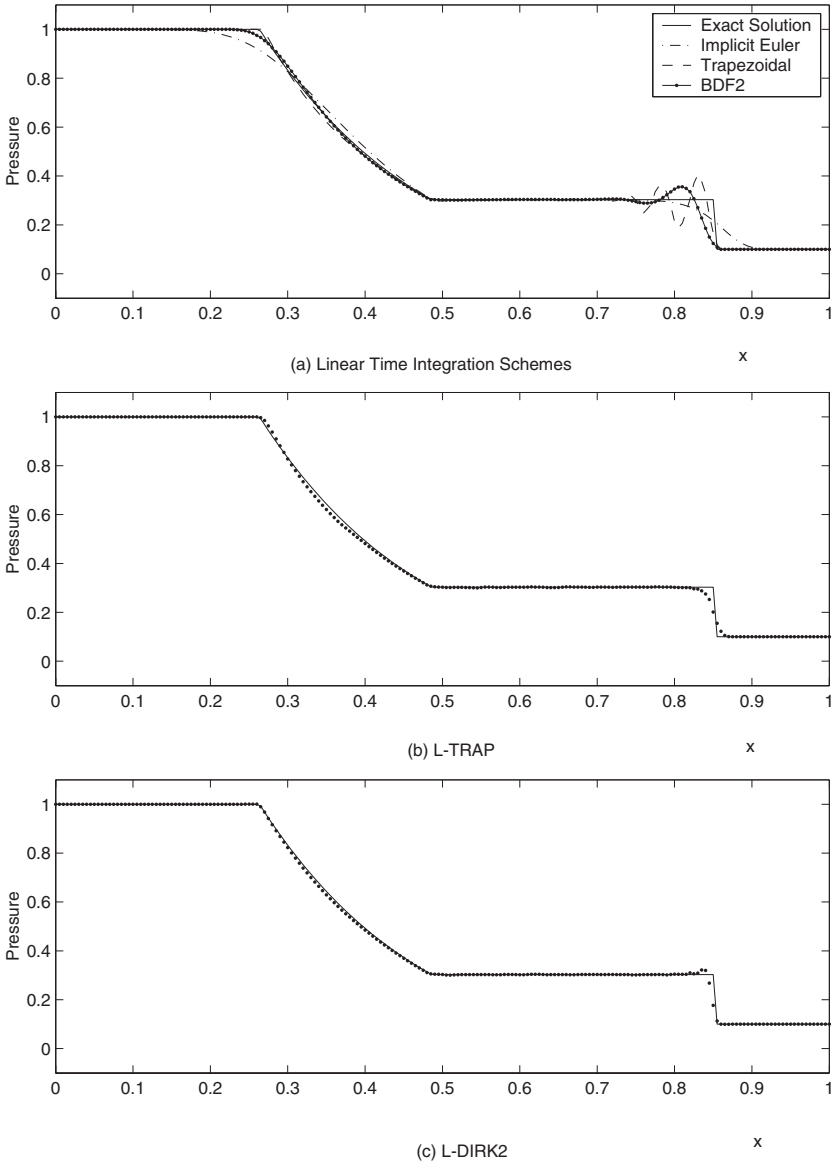

Fig. 8. Sod's problem (Pressure), $\sigma = 3.0$, 2nd order MUSCL, $N = 200$, $t = 0.2$.

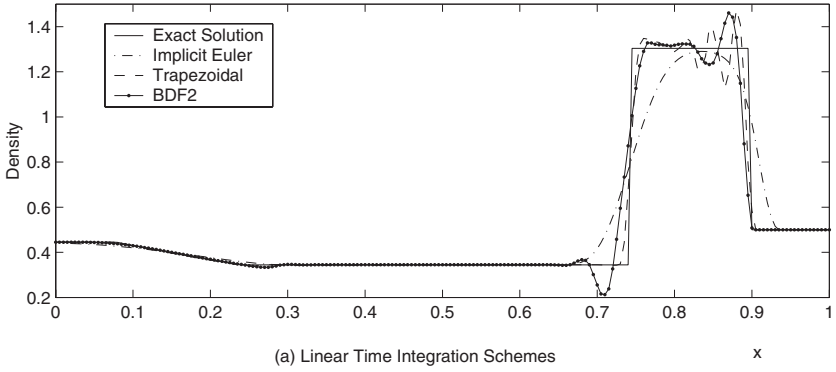

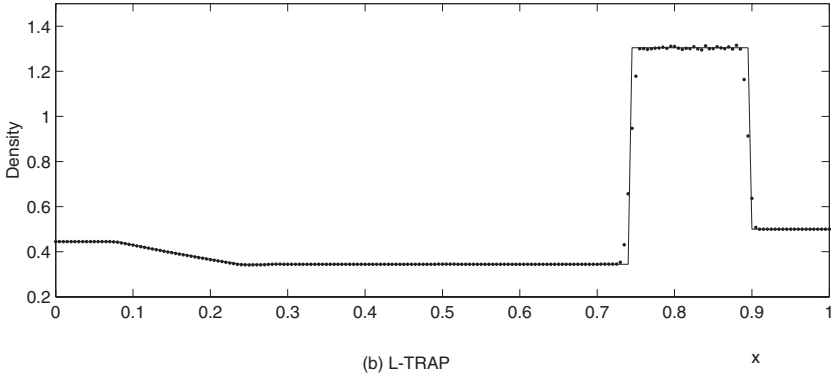

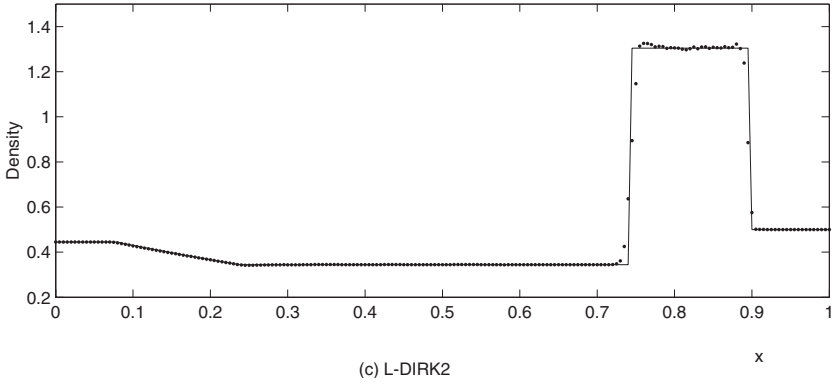

Fig. 9. Lax's problem (Density), $\sigma = 3.0$, 2nd order MUSCL, $N = 200$, $t = 0.16$.

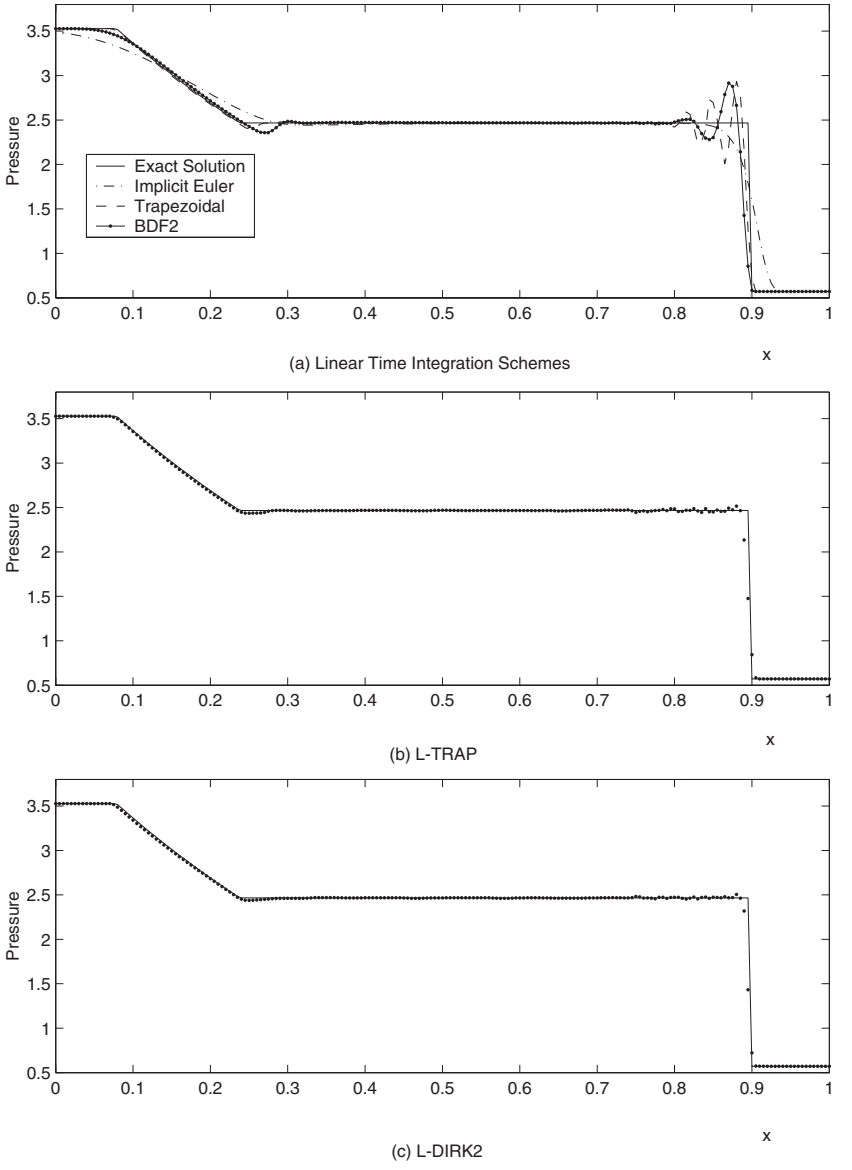

Fig. 10. Lax's problem (Pressure), $\sigma = 3.0$, 2nd order MUSCL, $N = 200$, $t = 0.16$.

function of the ratio of successive θ_j. Hence, a better limiter would correspond to a smoother distribution of θ_j over the domain.

6. CONCLUSION

A new class of time-limited non-oscillatory implicit schemes have been introduced. The main concept behind these schemes is that the order of accuracy in time is dropped locally in regions where the time evolution of the solution is not smooth. Hence, these schemes are essentially *non-linear in time* and can thus circumvent the limits imposed on linear time integration schemes. Numerical results obtained from the solution of scalar and systems of conservation laws have demonstrated that such a concept can work and that it is a promising area of research.

There is a lot to learn from monotonicity concepts that are used in spatial discretization in the sense that these concepts can be extended to time integration. A number of improvements can be made to the present schemes. The L-TRAP and L-DIRK2 schemes are general and there are many ways by which one could improve the design θ_j (a monotone time interpolation approach is used in this work) and $\theta_{j+\frac{1}{2}}$ (a simple average has been used).

Overall, we have demonstrated that these schemes, when used with high order spatial discretizations yield non-oscillatory solutions for much larger time-steps as compared to linear time integration schemes. It has to be mentioned that further research is required before these schemes can be successfully applied to actual applications in computational physics. This paper serves just an introduction to the concepts of applying limiters to linear high order time integration schemes.

APPENDIX A. TVD LIMITS OF SOME IMPLICIT SCHEMES

We consider expressing TVD limits for implicit schemes as a ratio of the explicit Euler TVD limit. This closely follows the approach in [1]. Consider an s-stage implicit Runge–Kutta (RK) scheme for Eq. (4):

$$u^{(i)} = u^n + \Delta t \sum_{j=1}^{i} a_{ij} L(u^{(j)}) \qquad i = 1 \cdots s$$

$$u^{n+1} = u^n + \sum_{i=1}^{s} b_i L(u^{(i)})$$

This is represented in the Butcher array form as:

$$\begin{array}{c|cccccc} c_1 & a_{11} & 0 & 0 & . & . & 0 \\ c_2 & a_{21} & a_{22} & 0 & . & . & 0 \\ . & . & . & . & . & . & . \\ . & . & . & . & . & . & . \\ c_s & a_{s1} & a_{s2} & a_{s3} & . & . & a_{ss} \\ \hline & b_1 & b_2 & b_3 & . & . & b_s \end{array}$$

Table III. Implicit Euler, Trapezoidal and SDIRK-2 ($\gamma = \frac{2-\sqrt{2}}{2}$)

0 | 0 0	0 | 0 0	γ | γ
1 | 0 1	1 | $\frac{1}{2}$ $\frac{1}{2}$	1 | $1-\gamma$ γ
1 | 0 1	1 | $\frac{1}{2}$ $\frac{1}{2}$	| $1-\gamma$ γ

with, $c_i = \sum_j a_{ij}$. For example, the implicit Euler, Trapezoidal and the 2-stage Singly Diagonally Implicit Runge–Kutta (SDIRK-2) methods are given in Table III.

For convenience of analysis, we write the above equation in the form,

$$u^{(0)} = u^n \tag{14}$$

$$u^{(i)} = \sum_{j=0}^{i-1} \alpha_{i,j} u^{(j)} + \Delta t \sum_{j=1}^{i} \beta_{i,j} L(u^{(j)}), \qquad i = 1 \cdots s+1 \tag{15}$$

$$u^{n+1} = u^{(s+1)} \tag{16}$$

Theorem. If a spatial discretization is TVD for $\Delta t \leqslant \Delta t_{ee}$ if used with an explicit Euler time discretization, then it will be TVD if used with the RK method (Eqs. (14)–(16)) under the new time step restriction,

$$\Delta t \leqslant k\, \Delta t_{ee}, \quad k = \min_{i,j} \frac{\alpha_{i,j}}{\beta_{i,j}}, \qquad i = 1 \cdots s+1, \quad j = 0 \cdots i-1.$$

Proof. Consider any stage in Eq. (16), and for the moment, assume $\alpha_{i,j} \geqslant 0$ and $\beta_{i,j} \geqslant 0$

$$u^{(i)} = \sum_{j=0}^{i-1} \alpha_{i,j} u^{(j)} + \Delta t \sum_{j=1}^{i} \beta_{i,j} L(u^{(j)}), \qquad i = 1 \cdots s+1$$

$$u^{(i)} + \beta_{i,i} u^{(i)} = \sum_{j=0}^{i-1} \alpha_{i,j} \left[u^{(j)} + \Delta t \frac{\beta_{i,j}}{\alpha_{i,j}} L(u^{(j)}) \right] + \beta_{i,i} [u^{(i)} + \Delta t\, L(u^{(i)})]$$

$$\| u^{(i)} + \beta_{i,i} u^{(i)} \| = \left\| \sum_{j=0}^{i-1} \alpha_{i,j} \left[u^{(j)} + \Delta t \frac{\beta_{i,j}}{\alpha_{i,j}} L(u^{(j)}) \right] + \beta_{i,i} [u^{(i)} + \Delta t\, L(u^{(i)})] \right\|$$

$$(1 + \beta_{i,i}) \| u^{(i)} \| \leqslant \sum_{j=0}^{i-1} \alpha_{i,j} \left\| \left[u^{(j)} + \Delta t \frac{\beta_{i,j}}{\alpha_{i,j}} L(u^{(j)}) \right] \right\| + \beta_{i,i} \| [u^{(i)} + \Delta t\, L(u^{(i)})] \|$$

$$\| u^{(i)} \| + \beta_{i,i} \| u^{(i)} \| \leqslant \sum_{j=0}^{i-1} \alpha_{i,j} \| u^{(j)} \| + \beta_{i,i} \| u^{(i)} \| \qquad \textbf{if} \quad \boldsymbol{\Delta t \leqslant k\, \Delta t_{ee}}$$

Therefore, $$\| u^{(i)} \| \leqslant \sum_{j=0}^{i-1} \alpha_{i,j} \| u^{(j)} \|$$

If this is applied recursively from $i = 0$ to $s+1$, we get

$$\|u^{(i)}\| \leqslant \sum_{j=0}^{i-1} \alpha_{i,j} \|u^{(n)}\|, \qquad i = 0 \cdots s+1$$

but, by consistency, $\sum_{j=0}^{i-1} \alpha_{i,j} = 1$. Therefore, we have,

$$\|u^{n+1}\| \leqslant \|u^n\|$$

It can also be shown that the assumption that $\beta_{i,j} \geqslant 0$ can be relaxed under certain conditions, but the positivity of the α 's cannot be relaxed [1]. Hence, Implicit RK schemes should try to maximize $\min_{i,j} \frac{\alpha_{i,j}}{\beta_{i,j}}$. Gottlieb, Shu, and Tadmor [2] have shown that unconditionally TVD implicit schemes of order higher than one do not exist.

A.1. θ Schemes

The implicit Euler and Trapezoidal schemes are given by the one-parameter family of schemes given by,

$$u^{n+1} = u^n + \Delta t[(1-\theta)\, L(u^n) + \theta L(u^{n+1})]$$

Hence, the TVD limit is given by,

$$k = \frac{1}{1-\theta}, \qquad \text{or} \qquad \Delta t \leqslant \Delta t_{ee} \frac{1}{1-\theta}$$

Hence, the implicit Euler scheme ($\theta = 1$), is unconditionally TVD ($k = \infty$) and the Trapezoidal scheme ($\theta = \frac{1}{2}$) is conditionally TVD ($k = 2$).

A.2. L-DIRK2 with Constant θ

Consider the L-DIRK2 scheme with a constant value of θ over the domain. Then, this scheme can be written in the Butcher array format given by,

γ	γ	
1	$\gamma+\theta(1-2\gamma)$	$(1-\gamma)+\theta(2\gamma-1)$
	$\gamma+\theta(1-2\gamma)$	$(1-\gamma)+\theta(2\gamma-1)$

In this case,

$$\begin{aligned}
\alpha_{10} &= 1 \\
\beta_{11} &= \gamma \\
\alpha_{20} &= 1-\alpha_{21} \\
\beta_{21} &= \gamma(1-\alpha_{21})+\theta(1-2\gamma) \\
\beta_{22} &= (1-\gamma)+\theta(2\gamma-1)
\end{aligned}$$

Hence, α_{21} is a parameter that can be varied, giving a TVD limit of:

$$\begin{aligned}\Delta t &\leqslant \frac{\alpha_{21}}{\beta_{21}} \Delta t_{ee} \\ &= \frac{\alpha_{21}}{\gamma(1-\alpha_{21})+\theta(1-2\gamma)} \Delta t_{ee} \\ &= k\, \Delta t_{ee}\end{aligned}$$

Where,

$$k = \frac{1}{\theta(1-2\gamma)} \qquad (\alpha_{21} = 1)$$

The 2-stage SDIRK scheme corresponds to $\theta = 1$ and is thus conditionally TVD with $k = \frac{1}{1-2\gamma} \approx 2.4142$.

ACKNOWLEDGMENT

Work done under NSF Grant DMS-0107218.

REFERENCES

1. Gottlieb, S., and Shu, C.-W. (1998). Total variation diminishing Runge–Kutta schemes. *Math. Comp.* **67**, 73–85.
2. Gottlieb, S., Shu, C.-W., and Tadmor, E. (2001). Strong stability preserving high order time discretization methods. *SIAM Rev.* **43**, 89–112.
3. Hairer, E., and Wanner, G. (1991). *Solving Ordinary Differential Equations*, Vol. 2, Springer-Verlag.
4. Harten, A. (1983). High resolution schemes for hyperbolic conservation laws. *J. Comput. Phys.* **49**, 357–393.
5. Harten, A., and Osher, S. (1987). Uniformly high order accurate non-oscillatory schemes 1. *SIAM J. Numer. Anal.* **24**.
6. Harten, A., Hyman, J., and Lax, P. (1976). On finite difference approximations and entropy conditions for shocks. *Comm. Pure Appl. Math.* **29**, 297–322.
7. Hyunh, H. (1993). Accurate monotone cubic interpolation. *SIAM J. Numer. Anal.* **30**, 57–100.
8. Laney, C. B. (1998). *Computational Gasdynamics*, Cambridge University Press.
9. Pulliam, T. (1993). *Time Accuracy and the Use of Implicit Methods*, AIAA Paper 93-3360.
10. Roe, P. (1985). Some contributions to the modelling of discontinuous flows. *Lectures Appl. Math.* **22**, 163–193.
11. Shu, C.-W. (1998). Essentially non-oscillatory and weighted essentially non-oscillatory schemes for hyperbolic conservation laws in advanced numerical approximation of nonlinear hyperbolic equations. In Cockburn, B., Johnson, C., Shu, C.-W., and Tadmor, E. (eds.), *Lecture Notes in Mathematics*, Vol. 1697, Springer, pp. 325–432.
12. Suresh, A., and Huynh, H. (1997). Accurate monotonicity-preserving schemes with Runge–Kutta time stepping. *J. Comput. Phys.* **136**.
13. Van Leer, B. (1979). Towards the ultimate conservative difference scheme v. a second order sequel to Godunov's method. *J. Comput. Phys.* **32**, 101–136.
14. Wada, W., and Liou, M.-S. (1997). An accurate and robust flux splitting scheme for shock and contact discontinuities. *SIAM J. Sci. Comput.* **18**, 633–657.
15. Yoon, S., and Jameson, A. (1988). Lower-upper symmetric Gauss–Seidel method for the Euler and Navier–Stokes equations. *AIAA J.* **26**, 1025–1026.